

## Triaxiality of the yrast states of odd-A Lu isotopes

Yu-sheng Liang,<sup>1,2,\*</sup> Xing-ju Wu,<sup>1,3,4</sup> Jin-zhang Xu,<sup>1,3</sup> Xing-qu Chen,<sup>1,2,3</sup> and Zheng Xing<sup>1,2,3</sup>

<sup>1</sup>Centre of Theoretical Nuclear Physics, National Laboratory of Heavy Ion Accelerator, Lanzhou 730000, People's Republic of China

<sup>2</sup>Shanghai Institute of Nuclear Research, Chinese Academy of Sciences, P.O. Box 800-204, Shanghai 201800, People's Republic of China<sup>†</sup>

<sup>3</sup>Department of Modern Physics, Lanzhou University, Lanzhou 730000, People's Republic of China

<sup>4</sup>Physics Department, Lu-an Teacher's College, Lu-an, Anhui 237012, People's Republic of China

(Received 17 May 1999; published 27 September 1999)

The energy spectra and electromagnetic transition probabilities of the negative-parity yrast states in odd-A Lu isotopes ( $Z=71$ ) are investigated systematically using the particle-rotor model and are compared with experimental data before and after the band crossing. It is noted that the moment of inertia of the core after the band crossing is as much a smooth function of the total angular momentum  $I$ , as that before the band crossing and can be described by the  $ab$  formula. Appreciably different are the triaxial deformations before ( $\sim -20^\circ$ ) and after ( $\sim +10^\circ$ ) the band crossing for  $^{161,163,165}\text{Lu}$ , while they are more or less similar ( $\sim -10^\circ$ ) for  $^{167}\text{Lu}$  determined from the calculation. [S0556-2813(99)03910-2]

PACS number(s): 21.60.Ev, 21.10.Re, 21.10.Ky, 27.70.+q

### I. INTRODUCTION

Many experiments have been done recently on high-spin spectroscopy of rare-earth nuclei, but our quantitative understanding of their nuclear structure, especially their shapes is not yet sufficient; on the other hand, most theoretical models can just deal with energy spectrum data leaving electromagnetic transition probabilities out of the account, thus their analyses are still incomplete and cannot explain shape changes. Among the odd- $Z$  heavy rare-earth nuclei around  $Z\sim 70$ , the lutetium isotopic chain of  $Z=71$  has typically had rich data [1–4]: the negative-parity yrast band spectra in  $^{161,163,165,167}\text{Lu}$ , their ratios of the reduced transition probabilities  $B(M1; I\rightarrow I-1)$  to  $B(E2; I\rightarrow I-2)$ , the dynamical quadrupole moments  $Q^{(2)}$  of the stretched  $E2$  transitions for  $^{163}\text{Lu}$  and the  $s$  band of  $^{161}\text{Lu}$ , and the ratio of the two kinds of dynamical quadrupole moments  $Q^{(1)}/Q^{(2)}$  for  $^{165}\text{Lu}$ , all have been measured. So a systematic study on the high-spin states of these odd-A Lu nuclei becomes feasible. Our interest is centered on whether these odd-A Lu isotopes are all triaxially deformed in their yrast states. Reference [5] presented systematic theoretical calculations on the yrast  $\pi[514]9/2$  band of  $^{161,163,165}\text{Lu}$  before band crossing. Reference [6] analyzed the yrast  $s$  band of  $^{165}\text{Lu}$  after band crossing. We see from those analyses that the  $\pi[514]9/2$  bands of  $^{161,163,165}\text{Lu}$  before band crossing are triaxial with  $\gamma\sim -20^\circ$ , and the  $s$  band of  $^{165}\text{Lu}$  after crossing is triaxial with  $\gamma\sim -10^\circ$ . Nevertheless, there are problems with these odd-A Lu nuclei.

(1) It has been interpreted that the  $\pi[660]1/2$  bands in  $^{163,165,167}\text{Lu}$  are triaxially superdeformed [2,7,8,14,15]. On the other hand, among the normal deformed bands of these nuclei, the negative-parity yrast  $\pi[514]9/2$  bands in  $^{161,163,165}\text{Lu}$  were understood as triaxial [5], and so it can be

asked whether the  $\pi[514]9/2$  band of  $^{167}\text{Lu}$  before band crossing is also triaxial?

(2) The  $s$  bands of  $^{161,163,167}\text{Lu}$  have not yet been studied, i.e., whether their yrast  $\pi[514]9/2$  bands are also triaxial after band crossing in addition to  $^{165}\text{Lu}$ [6]? On the other hand, the  $^{165}\text{Lu}$  ( $s$  band) data of  $B(M1; I\rightarrow I-1)/B(E2; I\rightarrow I-2)$  used in the analysis of Ref. [6] were taken before publication [3], but some data revision in Ref. [3] is now available.

(3) The calculations of Refs. [5,6] utilized a hydrodynamical type moment of inertia:

$$J_k = \frac{4}{3} J_0(I) \sin^2\left(\gamma + k \frac{2\pi}{3}\right), \quad k=1,2,3, \quad (1)$$

where  $J_k$  is the moment of inertia associated with rotation about the intrinsic  $k$ th axis, and  $J_0 = J_0(I)$  is variable vs spin  $I$  to fit the experimental spectrum, but there was not a clear analytical form given of the relation between  $J_0$  and spin  $I$ .

(4) For years, the ideal rigid rotor model was used as the approximation to the zeroth order for rotation motion, but the deviation of its rotational energy spectrum formula,  $E(I) = AI(I+1)$ , from observed data of rotational bands had been found at different nuclear regions to a different extent. A much better formula of only two parameters for rotational energy spectrum was deduced phenomenologically [9], and derived theoretically from a Bohr Hamiltonian [10], and is now often called the  $ab$  formula:

$$E(I) = a[\sqrt{1+bI(I+1)} - 1] = \frac{\hbar^2}{2J_0(I)} I(I+1), \quad (2)$$

in which is included also the idea of a variable moment of inertia  $J_0(I)$ :

$$J_0(I) = J_{00} \frac{1 + \sqrt{1+bI(I+1)}}{2}. \quad (3)$$

\*Corresponding author. Electronic address: liangysh@public1.sta.net.cn

<sup>†</sup>Corresponding address.

This  $ab$  formula can describe satisfactorily all rotational spectra of ground-state bands of the normal deformed even-even nuclei in rare-earth and actinide regions [10,11]. It has been proved recently that the transition energy spectra of superdeformation bands can also be excellently reproduced by this  $ab$  formula, Eq. (2), and the moment-of-inertia  $J_0$ , Eq. (3), derived from Eq. (2) [12–15]. Thus Eq. (3) offers a smooth function between  $J_0$  in Eq. (1) and the total angular momentum  $I$ . But there are not yet calculated the yrast  $s$  (upper)-band spectra with Eqs. (2) and (3). What about the situation of applying this  $ab$  formula and its derivative moment-of-inertia Eq. (3) to various excited rotational bands in high-spin states, especially, to the yrast  $s$  band after the band-crossing region? It seems that no such systematic investigation has been done, to our knowledge.

Here we shall calculate both the energy spectra and transition probabilities of the negative-parity yrast states of odd- $A$  Lu-isotopes using the particle-rotor model, and then compare our results with experimental data in order to clarify the above points, particularly to study the change of triaxiality both before and after the band crossing of the yrast  $\pi[514]9/2$  bands in the  $^{161,163,165,167}\text{Lu}$   $Z=71$  isotopic chain, and at the same time to test the applicability of Eqs. (2) and (3) to the yrast spectrum region of the  $s$  band, i.e., after band crossing.

## II. THE MODEL

Based on the experimental level schemes [1–4], the last proton in these odd- $A$  Lu nuclei occupies the yrast  $\pi[514]9/2$  orbital with negative parity, which is not mixed up with neighboring orbitals of positive parity. To investigate these yrast states, we use the single- $j$  particle-triaxial-rotor model [5,6] to calculate both the energy spectra and the transition probabilities before and after the band crossing. There is only one quasiproton in the  $h_{11/2}$  subshell coupled with the even-even core before band crossing, whereas two  $i_{13/2}$  neutrons are aligned by the rotation after crossing, thus three quasiparticles are coupling with the core. If the angular momentum of the odd-proton is expressed as  $\vec{j}_p$ , the neutron spin alignment as  $\vec{J}_n$ , and the collective angular momentum of the even-even core as  $\vec{R}$ , then the total angular momentum  $\vec{I} = \vec{R} + \vec{J}_n + \vec{j}_p$ . To deal with this  $s$  band after band crossing, our total Hamiltonian is written as a sum of the rotor part and the intrinsic parts for the quasineutrons and quasiproton:

$$H = H_{\text{rot}} + H_{\text{intr},n} + H_{\text{intr},p}. \quad (4)$$

Here the triaxial-rotor Hamiltonian is given by

$$H_{\text{rot}} = \sum_{k=1}^3 \frac{\hbar^2}{2J_k} (\vec{R})_k^2 = \sum_{k=1}^3 \frac{\hbar^2}{2J_k} [(I_k - J_{nk}) - j_{pk}]^2, \quad (5)$$

in which  $R_k$  is the collective angular momentum of the even-even core,  $J_k$  is the moment of inertia associated with rotation about the intrinsic  $k$ th axis. In numerical calculations, we also take the moment of inertia of the hydrodynamical type, Eq. (1), in which  $J_0(I)$  of Eq. (3), derived from the  $ab$

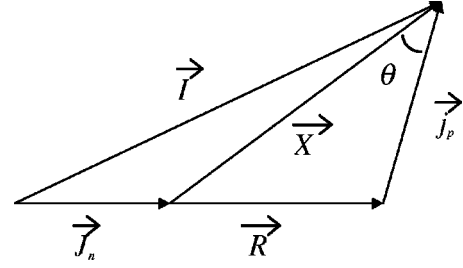


FIG. 1. Geometric relation of the coupling angular momenta of the  $s$  band: the total angular momentum  $\vec{I}$ , the  $s$  band neutron spin-alignment  $\vec{J}_n$ , the rotor collective angular momentum  $\vec{R}$ , and the odd quasiproton angular momentum  $\vec{j}_p$ .

formula, Eq. (2), is used as the function vs spin  $I$ , wherein parameters  $J_{00}$  and  $b$  are estimated by fitting the  $\gamma$ -transition energy spectrum.

It is not practical to perform a numerical calculation of the particle-rotor model with the three-quasiparticle states because of the large configuration space. Due to the one-particle character of the electromagnetic transition operators, the change in the number of quasiparticles does not have any influence on the signature-dependent part of the transition-matrix elements and on the nuclear shape. We can freeze the intrinsic degrees of freedom of the aligned neutrons, just as the simplified model proposed by Ref. [6] did to deal with the  $s$  band configuration. Since at present we are especially interested in the spin region of the  $s$  band in which the neutron spin alignment is nearly constant, viz.,  $J_n \approx 10$ , then the contribution from the intrinsic Hamiltonian of the aligned neutrons is an additional constant, and this intrinsic term  $H_{\text{intr},n}$  in Eq. (4) can be ignored as done in Ref. [6]. Here we can also assume that  $\vec{J}_n$ , the neutron-spin alignment of the  $s$  band, is parallel with  $\vec{R}$ , the collective angular momentum of the (triaxial) core, then an angular momentum for the  $s$  band  $\vec{X}$ , can be defined as in Ref. [6]:

$$\vec{X} = \vec{I} - \vec{J}_n = \vec{R} + \vec{j}_p. \quad (6)$$

The coupling scheme of the angular momenta in the  $s$  band is shown in Fig. 1.

Thus the three-quasiparticle problem of the total Hamiltonian (4) of the  $s$  band is reduced to a one-quasiparticle problem quite similar to that of the usual  $g$  band with only the odd-proton intrinsic Hamiltonian  $H_{\text{intr},p}$ :

$$H = \sum_{k=1}^3 \frac{\hbar^2}{2J_k} (\vec{R})_k^2 + H_{\text{intr},p}, \quad (7)$$

which is of the usual form of one-quasiparticle configuration and is easy to be diagonalized. This Hamiltonian can be used for both the  $g$  band ( $J_n = 0$ ,  $\vec{X} = \vec{I}$ ,  $\vec{R} = \vec{I} - \vec{j}_p$ ) and the  $s$  band ( $J_n \approx 10$ ,  $\vec{X} = \vec{I} - \vec{J}_n$ ,  $\vec{R} = \vec{X} - \vec{j}_p$ ), the only difference is that the rotor angular momentum of the  $s$  band is calculated as  $\vec{R} = \vec{X} - \vec{j}_p$ . The detailed formulas necessary for the calculation in the particle-rotor model can be found in Refs. [6,13].

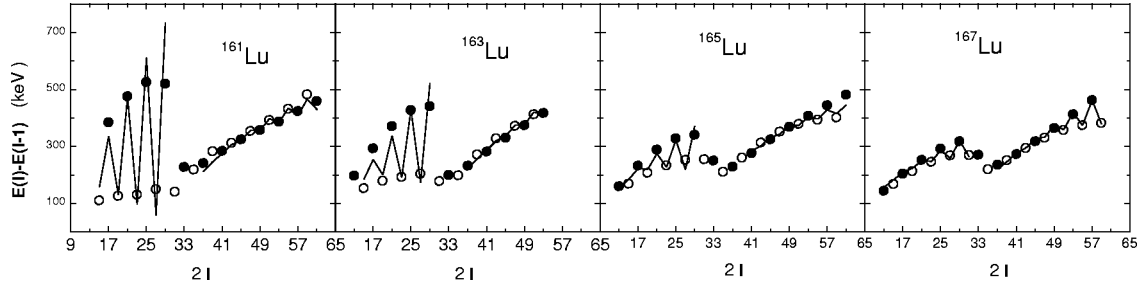


FIG. 2. Energy difference  $\Delta E = E(I) - E(I-1)$  versus spin  $I$  of the states in the  $[514]9/2^-$  band of the odd-Lu chain. The experimental data (from Refs. [1–4]) are shown as solid circles (corresponding to the energy difference from the state with signature  $\alpha = +1/2$  to  $\alpha = -1/2$ ), and open circles (corresponding to the energy difference from the state with signature  $\alpha = -1/2$  to  $\alpha = +1/2$ ). The calculated values are connected by the solid lines. The parameters used in the particle-(triaxial)-rotor model calculation before (after) band crossing for  $^{161}\text{Lu}$ ,  $^{163}\text{Lu}$ ,  $^{165}\text{Lu}$ ,  $^{167}\text{Lu}$ , respectively, are  $\gamma = -21^\circ (+14^\circ)$ ,  $-18^\circ (+14^\circ)$ ,  $-15^\circ (+9^\circ)$ ,  $-14^\circ (-10^\circ)$ ;  $\Delta/\kappa = 0.55(0.55)$ ,  $0.45(0.45)$ ,  $0.40(0.40)$ ,  $0.40(0.40)$ ;  $\lambda/\kappa = 0.40(0.40)$ ,  $0.40(0.40)$ ,  $0.40(0.40)$ ,  $0.50(0.50)$ ;  $J_{00}\kappa = 35(66)$ ,  $50(65)$ ,  $55(58)$ ,  $68(68)$ ;  $b \times 10^3 = 5.5(2.3)$ ,  $4.5(1.5)$ ,  $8.5(5.5)$ ,  $5.0(2.5)$ . Here  $\kappa$  is used as an energy unit which is determined by normalizing the calculated values of  $\gamma$ -transition energies to one of the  $\gamma$ -transition energy data,  $\kappa$  is about 2–2.5 MeV in our interested nuclear region.

The dynamical quadrupole moments  $Q^{(1)}$  and  $Q^{(2)}$  are extracted separately from their related  $B(E2)$  values using the following formula:

$$B(E2; I \rightarrow I-p) = \frac{5}{16\pi} \langle IK20 | I-pK \rangle^2 Q^{(p)^2}, \quad p=1,2. \quad (8)$$

By writing the total angular momentum  $\vec{I}$  as  $\vec{I} = \vec{R} + \vec{J}_n + \vec{j}_p = \vec{R}' + \vec{j}_p$ , where  $\vec{R}' \equiv \vec{R} + \vec{J}_n$ , the magnetic-dipole operator  $\vec{\mu}$  is expressed as in Ref. [6]:

$$\vec{\mu} = g_R \vec{R} + g_{J_n} \vec{J}_n + g_{j_p} \vec{j}_p = g_R \vec{I} + (g_{j_p} - g_R) \vec{j}_p, \quad (9)$$

where

$$g_R' \equiv (g_R R + g_{J_n} J_n) / (R + J_n) = g_R + (g_{J_n} - g_R) J_n / R'. \quad (10)$$

The  $M1$  transition operator is reduced to the usual one employed in Refs. [5,6,13].

The Hamiltonian, Eq. (7), is diagonalized by using the BCS one-quasiparticle states for the particle wave functions. Using the resulting wave functions,  $B(M1)$  and  $B(E2)$  values can be calculated.

### III. RESULTS AND DISCUSSION

The calculation in the spin region before the band crossing is performed as usual with the particle-triaxial rotor model. Since after the band crossing, the  $s$  band is known to consist of  $(i_{13/2})^2$  quasineutrons, their alignment  $J_n \approx 10$  and  $g_{J_n} = -0.20$  are used in the calculation of this simplified model, Eq. (7).

The calculated energy difference  $E(I) - E(I-1)$  and the ratio of reduced transition probabilities  $B(M1)/B(E2)$  are compared with measured values for the negative-parity yrast  $\pi[514]9/2^-$  band of  $^{161,163,165,167}\text{Lu}$  in Figs. 2. and 3. The same  $B(M1)/B(E2)$  calculation of  $^{163}\text{Lu}$  with different  $Q_0$  parameter values for the  $g$  band and  $s$  band are shown in Fig. 4 for comparison. The calculated stretched  $E2$  transition moments  $Q^{(2)}$  for  $^{161}\text{Lu}$  and  $^{163}\text{Lu}$  are compared with data in

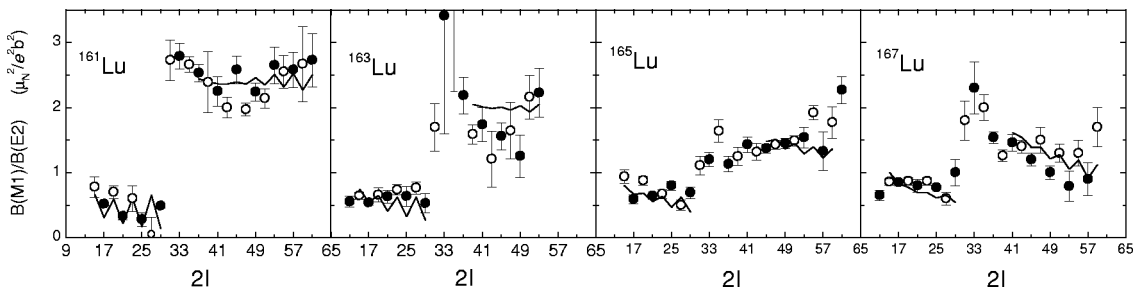


FIG. 3.  $B(M1; \Delta I=1)/B(E2; \Delta I=2)$  versus spin  $I$  of the states in the  $[514]9/2^-$  band of the odd-Lu chain. Experimental values with error bars (taken from Refs. [1–4]) are shown as solid circles (corresponding to the energy difference from the state with signature  $\alpha = +1/2$  to  $\alpha = -1/2$ ), and open circles (corresponding to the energy difference from the state with signature  $\alpha = -1/2$  to  $\alpha = +1/2$ ). Theoretical values are connected by solid lines. The parameters used for  $^{161}\text{Lu}$ ,  $^{163}\text{Lu}$ ,  $^{165}\text{Lu}$ ,  $^{167}\text{Lu}$ , respectively, are intrinsic quadrupole moment squared  $Q_0^2(e^2b^2) = 20, 25, 30.3, 36$ ; parameters of the particle-rotor model used in Fig. 2 are also used here; besides, several other parameters are used for transition probability calculation: equivalent electric charge  $e_{\text{eff}} \langle j | r^2 | j \rangle / Q_0 = 0.20e$ , and  $g_I = 1.0$ ,  $g_s = 3.91$ ,  $g_R = 0.42$ , while  $g_{J_n} = -0.20$ , and  $J_n = \begin{cases} 0 & \text{before band crossing} \\ 10 & \text{after band crossing} \end{cases}$ .

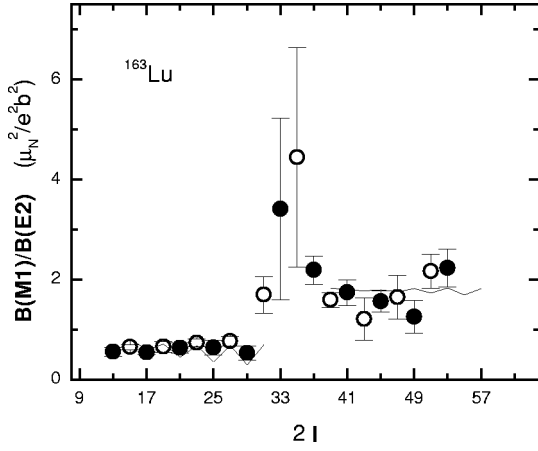


FIG. 4.  $B(M1; \Delta I=1)/B(E2; \Delta I=2)$  versus spin  $I$  of the states in  $[514]9/2^-$  band of  $^{163}\text{Lu}$ . Experimental values with error bars (taken from Refs. [2]) are shown using the same symbols as Fig. 3. Theoretical values are connected by solid lines. Parameters are the same as used in Fig. 3 except  $Q_0^2=23$  (for the  $g$  band), but 28 (for the  $s$  band) ( $e^2b^2$ ).

Figs. 5 and 6. The calculated  $Q^{(1)}/Q^{(2)}$  ratio of two kinds of dynamical quadrupole moments, with data of the negative-parity yrast band in  $^{165}\text{Lu}$ , are shown in Fig. 7.

From the good agreement of the calculated values with the observed ones, we can see the following.

(1) The apparent signature splittings of the energies before band crossing are decreasing when the neutron number of the isotope increases, whereas after band crossing these signature splittings of energies are not all large along the whole isotopic chain. Comparing the calculated signature splitting of the energies with the observed values, parameters of the particle-rotor model are chosen before and after the band crossing so that the observed data are, on the average, reproduced as well as possible.

Using the same parameters, the calculated ratios of  $B(M1; I \rightarrow I-1)$  to  $B(E2; I \rightarrow I-2)$  of these Lu isotopes, the transition quadrupole moments  $Q^{(2)}$  of  $^{161}\text{Lu}$  and  $^{163}\text{Lu}$ , and the ratio of dynamical quadrupole moments  $Q^{(1)}/Q^{(2)}$  of

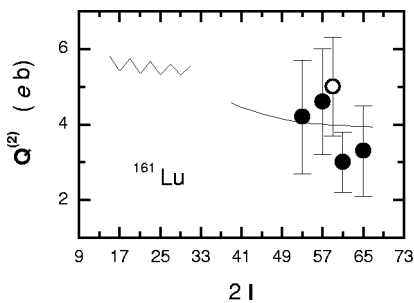


FIG. 5. The dynamical quadrupole moments  $Q^{(2)}$  versus spin  $I$  in the states of  $^{161}\text{Lu}$  yrast  $[514]9/2^-$  band. Experimental values for the  $s$  band with error bars (taken from Ref. [1]) are shown using the same symbols as those in Figs. 2 and 3. No experimental data for the  $g$  band is published yet. Theoretical values are connected by solid lines. Parameters are the same as used in Fig. 3.

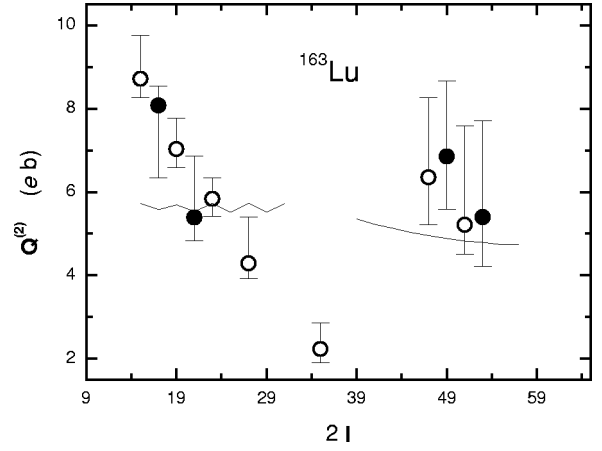


FIG. 6. The dynamical quadrupole moments  $Q^{(2)}$  versus spin  $I$  in the states of  $^{163}\text{Lu}$  yrast  $[514]9/2^-$  band. Experimental values with error bars (taken from Ref. [2]) are shown using the same symbols as those in Figs. 2 and 3. Theoretical values are connected by solid lines. Parameters are the same as used in Fig. 3 except  $Q_0^2=23$  (for the  $g$  band), but 28 (for the  $s$  band) ( $e^2b^2$ ).

$^{165}\text{Lu}$  agree quite well with observed ones, so the adopted parameters are reasonable.

The triaxiality  $\gamma$  values for  $\pi[514]9/2^-$  band before (after) the band crossing are  $-21^\circ(+14^\circ)$ ,  $-18^\circ(+14^\circ)$ ,  $-15^\circ(+9^\circ)$ , and  $-14^\circ(-10^\circ)$  in  $^{161,163,165,167}\text{Lu}$ , respectively. The symbol of the  $\gamma$  value is determined mainly to reproduce transition probabilities. Thus the triaxial deformations  $|\gamma|$  of these yrast bands are decreasing gradually before band crossing when the neutron number increases in the Lu isotopes, while  $\gamma$  values become positive after band crossing in  $^{161,163,165}\text{Lu}$ , i.e., their triaxial shapes change apparently before and after band crossing. But the  $\gamma$  value of  $^{167}\text{Lu}$  does not change much and keeps negative before and after band crossing, this also indicates that the  $^{167}\text{Lu}$  nucleus is the most rigid one among these Lu isotopes.

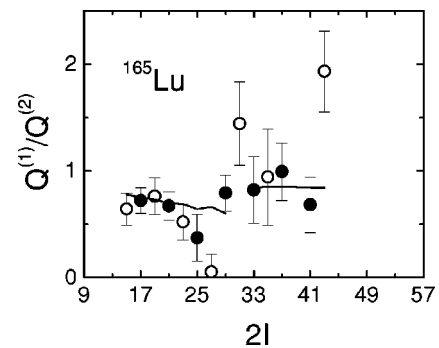


FIG. 7. The ratio of dynamical quadrupole moments  $Q^{(1)}/Q^{(2)}$  versus spin  $I$  in the states of the  $^{165}\text{Lu}$  yrast  $[514]9/2^-$  band. Experimental values with error bars (taken from Ref. [3]) are shown as solid circles (corresponding to the energy difference from the state with signature  $\alpha=+1/2$  to  $\alpha=-1/2$ ), and open circles (corresponding to the energy difference from the state with signature  $\alpha=-1/2$  to  $\alpha=+1/2$ ). Theoretical values are connected by solid lines. Parameters are the same as used in Fig. 3.

(2) The calculated energy spectra, Fig. 2, coincide with the observed data. This shows that the variation of the moment-of-inertia of the even-even core,  $J_0(I)$ , against angular momentum  $I$  can be well described by Eq. (3) both before and after band crossing, but with different  $J_{00}$  and  $b$  values, because the two different rotational bands are related. In our case, values of parameter  $b$  after band crossing are all smaller than those before band crossing, this is an indication that the moment of inertia  $J_0(I)$  varies faster versus spin  $I$  ( $g$  band) before band crossing than after crossing ( $s$  band).

For a given fixed  $\gamma$  value, the moment of inertia  $J_0(I)$  is a smoothly increasing function of spin  $I$ , which is reasonable since  $I$  dependence comes mainly from the decrease of the neutron pairing correlation as  $I$  increases. This variability of the moment of inertia  $J_0(I)$  of the core rotation in expression (3) is deduced from the  $ab$  formula, Eq. (2). Therefore, the  $ab$  formula can be used to study not only the  $g$  band but also the  $s$  band. This is a first successful example in the systematic study of  $s$  bands in high-spin states after band crossing using the variable moment of inertia, Eq. (3), of the  $ab$  formula, Eq. (2).

(3) The good agreement of the calculated values with experimental data also shows that the simplified model [6], Eq. (7), dealing with  $s$ -band configuration is a good approximation: The angular momenta of the two rotation-aligned quasineutrons  $\vec{J}_n$  can be assumed constant ( $J_n \simeq 10$  in the  $s$  band), and in parallel with  $\vec{R}$ , the collective angular momentum of the core. Then we can freeze the degrees-of-freedom of two aligned quasineutrons, i.e., neglect their intrinsic term in the total Hamiltonian (4), thus the 3qp problem, Eq. (4), is reduced to a 1qp problem, Eq. (7).

Using this simplified model, Eq. (7), for  $s$ -band configuration, the  $I$  dependence of the  $g$  factor of the core rotation,  $g_{R'}$ , is estimated from expression (10), Ref. [6]. The ‘‘step rise’’ increase of the magnitudes of the  $B(M1; I \rightarrow I-1)/B(E2; I \rightarrow I-2)$  ratios from the  $I$  region before the band crossing to the one after is well reproduced in Fig. 3. By examining the calculated results, one notes that this rise comes essentially from the increase of  $B(M1; I \rightarrow I-1)$  values due to the falling of  $g_R$  (before band crossing) to  $g_{R'}$  after band crossing, while the  $B(E2; I \rightarrow I-2)$  values do not have any essential change before and after the band crossing.

(4) By a careful comparison of theoretical values with observed ones in Fig. 3, we see that  $B(M1)/B(E2)$  calculated values for the  $s$  band in  $^{163}\text{Lu}$  are larger than the average of the experimental data. This is because parameter  $Q_0^2$  was taken as having the same value  $25(e^2b^2)$  before and after the band crossing in the calculation. On account of the change of nuclear shape after band crossing, the intrinsic quadrupole moment  $Q_0$  of the  $s$  band should also differ from that of the  $g$  band. If we increase the value for  $Q_0$  appropriately, the theoretical  $B(M1)/B(E2)$  values for the  $s$  band of  $^{163}\text{Lu}$  could fit the data much better (this is shown in Fig. 4), where  $Q_0^2=23$  (for the  $g$  band) and 28 (for the  $s$  band)

( $e^2b^2$ ) are used separately. When the same parameters are kept to calculate the dynamical quadrupole moments  $Q^{(2)}$  for  $^{163}\text{Lu}$  shown in Fig. 6, we could not fit the experimental values well, especially in the  $g$  band, where the data seem to mean a drastic change of its quadrupole deformation. To understand this phenomenon,  $Q^{(2)}$  experimental data with good accuracy for  $^{161,165,167}\text{Lu}$  are indispensably required.

The  $B(M1)/B(E2)$  data of the  $s$  band in  $^{165}\text{Lu}$  rise distinctly after  $I > 53/2$ . That feature was not reproduced by the present calculation, Fig. 3, but might be due to a decrease [3] in collectivity of the  $s$  band. The feature could be reproduced if a variable intrinsic quadrupole moment  $Q_0$ , which decreases versus spin  $I$ , is introduced in the calculation. More complete experimental data of transition probabilities, say, absolute  $Q^{(2)}$  and  $Q^{(1)}$  values of a chain of isotopes even like these Lu nuclei, which have already had comparatively rich data, are still needed to attain more reliable knowledge of the change of their nuclear shapes.

(5) Because of strong mixing between the  $g$  band and  $s$  band in the band crossing, our model is not applicable in this spin region, so there was no calculation done in the states with spin between  $I \sim \frac{29}{2} - \frac{41}{2}$ .

#### IV. SUMMARY

Energy spectra and transition probabilities of negative-parity yrast states of odd- $A$  Lu isotopes ( $Z=71$  chain) are investigated using the particle-rotor model. From the good agreement of theoretical values with experimental data, we can conclude the following.

(1) These yrast bands of odd-Lu isotopic chain  $^{161,163,165,167}\text{Lu}_{90,92,94,96}$  with negative parity are triaxially deformed before and after band crossing: the  $\gamma$  deformation changes from  $-21^\circ$  to  $-14^\circ$  (in the  $g$  band) before band crossing as the neutron number  $N$  increases, but the  $\gamma$  value changes from  $+14^\circ$  to  $-10^\circ$  (in the  $s$  band) after band crossing.

(2) Freezing the degrees-of-freedom of the aligned quasineutrons of the  $s$  band, the complicated 3qp problem, Eq. (4), is reduced to a 1qp problem, Eq. (7). This simplified model is a good approximation to the  $s$  band.

(3) The  $ab$  formula of only two parameters, Eq. (2), which depicts well ground-state rotational bands of axially symmetric even-even nuclei and gives properly the variation of their moment-of-inertia  $J_0(I)$  against angular momentum  $I$ , can also describe properly the variable relation of the moment-of-inertia  $J_0(I)$  versus spin  $I$  of their triaxially shaped core of odd- $A$  nuclei in their  $s$  bands.

#### ACKNOWLEDGMENTS

This work was supported by the National Natural Science Foundation of China under Grant Nos. 19575025 and 19075065, and by the Science Foundation of Nuclear Industry of China under Grant No. Y7197AY103.

- [1] C.-H. Yu, M. A. Riley, J. D. Garrett, G. B. Hagemann, J. Simpson, P. D. Forsyth, A. R. Mokhtar, J. D. Morrison, B. M. Nyakó, J. F. Sharpey-Schafer, and R. Wyss, Nucl. Phys. **A489**, 437 (1988); C.-H. Yu, F. K. McGowan, I. Y. Lee, J. D. Garrett, W. B. Gao, H. Q. Jin, N. R. Johnson, J. Lewis, S. Pilotte, L. L. Riedinger, J. C. Wells, and H. Xie, in *Proceedings of the International Conference on High Spin Physics and Gamma-soft Nuclei*, 1990, Pittsburgh, edited by J. X. Saladin *et al.* (World Scientific, Singapore, 1991); C.-H. Yu (private communication).
- [2] W. Schmitz, C. X. Yang, H. Hübel, A. P. Byrne, R. Müsseler, N. Singh, K. H. Maier, A. Kuhnert, and R. Wyss, Nucl. Phys. **A539**, 112 (1992); W. Schmitz *et al.* Phys. Lett. B **303**, 230 (1993); W. Schmitz, Ph.D. thesis, Bonn University, 1992; H. Hübel (private communication).
- [3] P. Frandsen *et al.*, Nucl. Phys. **A489**, 508 (1988).
- [4] C.-H. Yu *et al.*, Nucl. Phys. **A511**, 157 (1990).
- [5] I. Hamamoto and H. Sagawa, Phys. Lett. B **201**, 415 (1988).
- [6] I. Hamamoto and B. Mottelson, Phys. Lett. **167B**, 370 (1986).
- [7] H. Schnack-Petersen *et al.*, Nucl. Phys. **A594**, 175 (1995).
- [8] C. X. Yang, X. G. Wu, H. Zheng, X. A. Liu, Y. S. Chen, C. W. Shen, Y. J. Ma, J. B. Lu, S. Wen, G. S. Li, S. G. Li, G. J. Yuan, P. K. Weng, and Y. Z. Liu, Eur. Phys. J. A **1**, 237 (1998).
- [9] P. Holmberg and P. O. Lipas, Nucl. Phys. **A117**, 552 (1968).
- [10] C. S. Wu and J. Y. Zeng, Commun. Theor. Phys. **8**, 51 (1987).
- [11] F. X. Xu, C. S. Wu, and J. Y. Zeng, Phys. Rev. C **40**, 2337 (1989).
- [12] C. S. Wu, J. Y. Zeng, Z. Xing, X. Q. Chen, and J. Meng, Phys. Rev. C **45**, 261 (1992).
- [13] X. Q. Chen and Z. Xing, J. Phys. G **19**, 1869 (1993).
- [14] Z. Xing, Z. X. Wang, and X. Q. Chen, Chin. Phys. Lett. **15**, 170 (1998).
- [15] Z. Xing, Z. X. Wang, X. Q. Chen, and J. Z. Xu, High Energy Phys. Nucl. Phys. (in Chinese) **22**, 545 (1998).